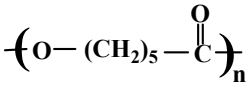

Poly(ε-caprolactone)

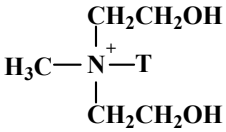

Methyl tallow bis-2-hydroxyethyl ammonium salt
(30B)

T: Tallow (~65%C18; ~30%C16; ~5%C14)

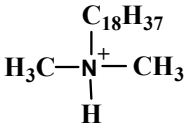

Dimethyl octadecyl ammonium salt
(C18)

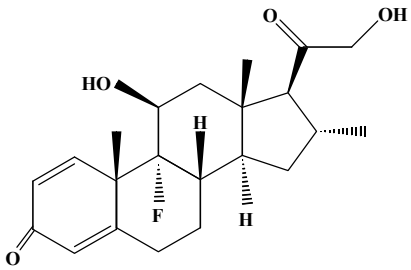

Dexamethasone

Scheme-1: The chemical structures of poly(ε-caprolactone), organic modifiers used in *C18* and *30B* nanoclays and dexamethasone.

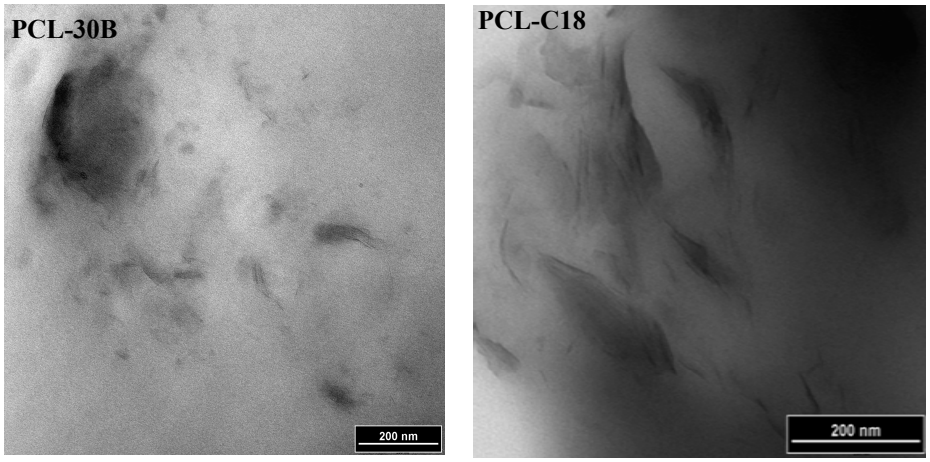

S1: Bright field transmission electron micrographs of nanocomposites (4 wt% clay) *PCL-30B* and *PCL-C18*, showing the well dispersed nanoclays in the *PCL* matrix The nanoclay stacks are obvious indicating the intercalated for both the nanohybrids.

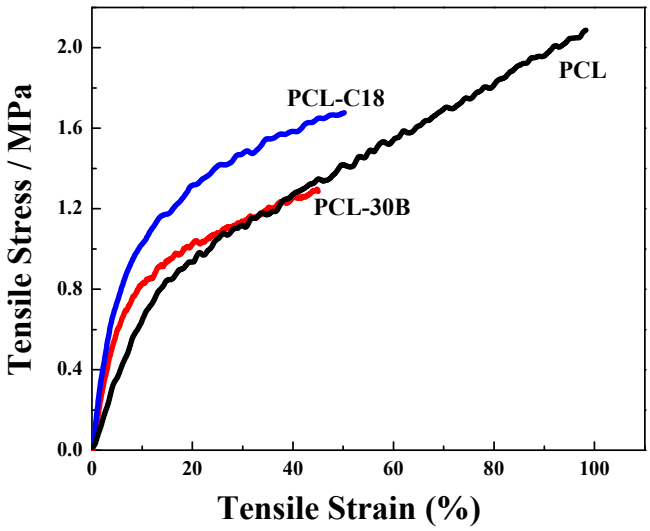

S2: Stress strain curve of *PCL* and its nanohybrids scaffolds. The tensile moduli, calculated from the initial linear slopes, have increased significantly for nanohybrid scaffolds as compared to pure *PCL* scaffolds. In addition, the toughness (area under the stress-strain curve) of *PCL-C18* scaffolds is higher than that of pure *PCL-30B* nanohybrid scaffolds

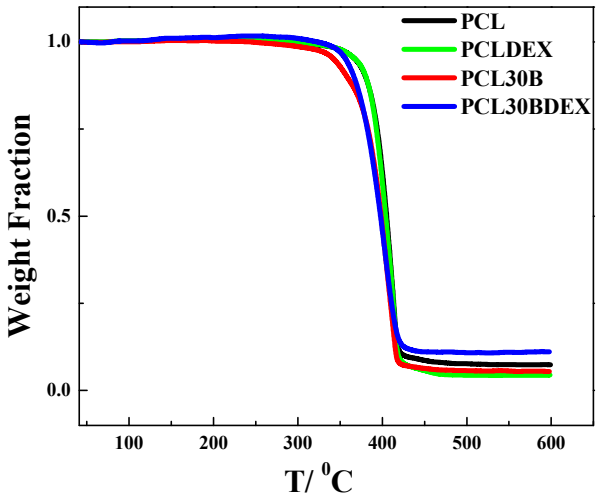

S3: *TGA* thermogramme of *PCL* and its respective nanohybrids, showing improved thermal stability after drug loading in pure *PCL* and its nanohybrids scaffolds *PCL-30B, PCL-C18.*

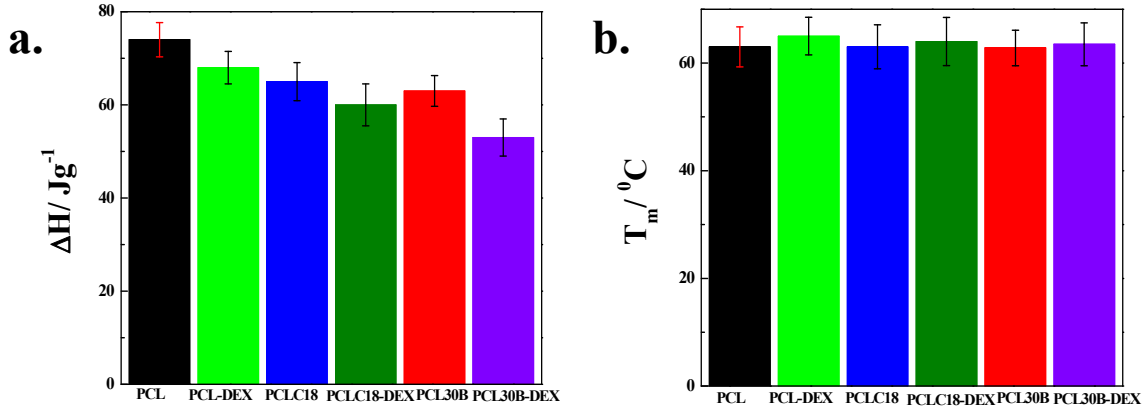

S4: a) Heat of fusion, b) melting point of with and without drug *DEX* loaded pure *PCL* and its nanohybrids. The heat of fusion of *PCL* scaffolds decrease after nanohybrids preparation and further drastically decrease after drug loading in pure *PCL* and its respective nanohybrids and decrement is highest in *PCL30B-DEX* showing the strong interaction between drug molecule with polymer as well as nanohybrids. *PCL* and its respective nanohybrids scaffold showing improved melting point after drug loading.

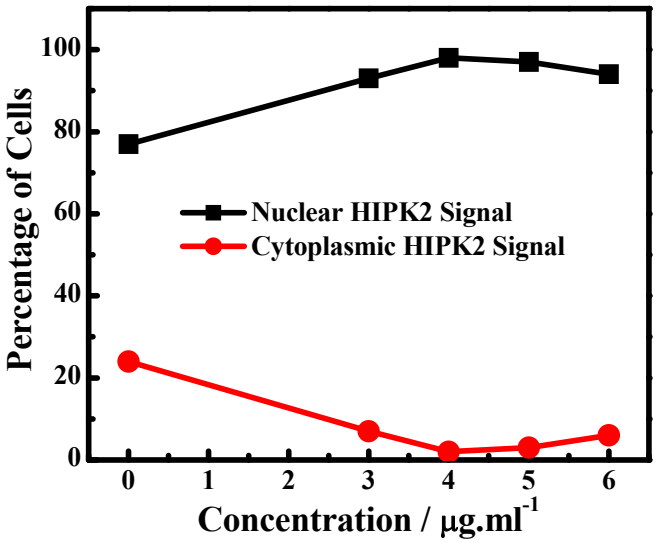

Figure S5: Shows the graphical representation of the effect of Cisplatin on the sub-cellular localization of pro-apoptotic activator, HIPK2. The cytoplasmic localization decreased with increase in the nuclear localized fraction in the concentration gradient of the chemotherapeutic agent. The percentage of both the cell types almost reaches a plateau at 4 and 5 μgml^{-1} concentration. On further increase of drug, the nucleus portion declines to some extent and vice-versa in the case of cytoplasmic one.

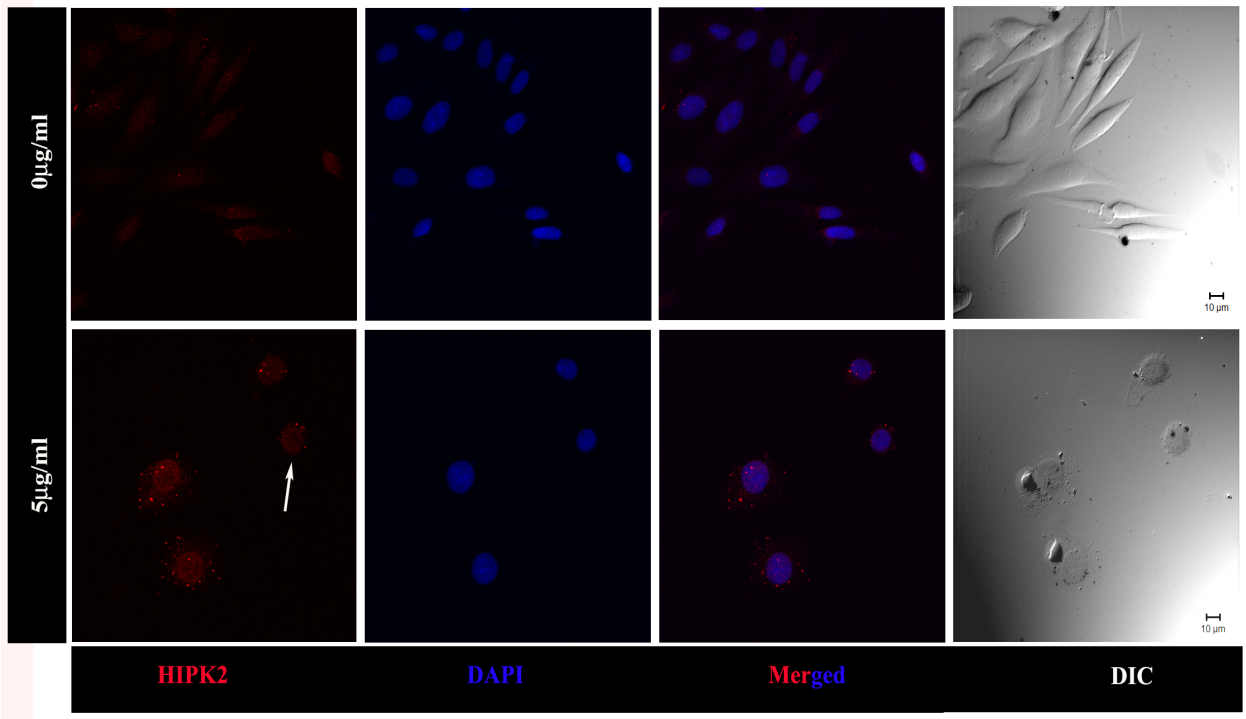

Figure S6: Presents the confocal section of SiHa cells showing the localization of HIPK2 in normal and stressed cells. In normal or unstressed cells (0µgml^{-1} of Cisplatin), HIPK2 can be seen localized mainly to the cytoplasm. Genotoxic stress induced through 5µgml^{-1} of Cisplatin resulted in nuclear localization of the protein. The negative control is devoid of any signal. DAPI (4'-6-diamidino-2-phenylidone dihydrochloride), was used for counterstaining. (Scale bar = 5µm)

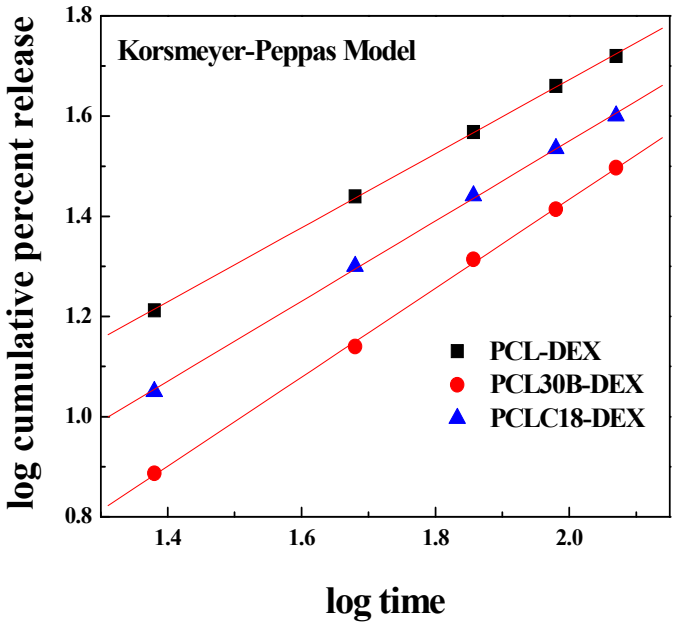

S7: Korsmeyer-Peppas model for mechanism of drug release in *PCL-DEX* and their respective nanohybrids *PCL30B-DEX, PCLC18-DEX.*

Table S1: Release rate constant (k), correlation coefficient (r^2) and diffusion release exponent (n) obtained using different mathematical models for drug loaded *PCL* and their respective nanohybrids.

Sample	Zero Order		First Order		Higuchi		Karsmeyer-Peppas	
	k	r^2	k	r^2	k	r^2	n	r^2
PCL-DEX	0.39 ± 0.014	0.988	0.0027 ± 0.0002	0.996	6.2 ± 0.2	0.997	0.74± 0.02	0.999
PCLC18-DEX	0.33 ± 0.016	0.976	0.0019 ± 0.0001	0.989	5.2 ± 0.2	0.988	0.80± 0.02	0.999
PCL30B-DEX	0.25 ± 0.025	0.986	0.0014 ± 0.0001	0.985	4.0 ± 0.4	0.992	0.89± 0.03	0.999